

Supporting Information

Fuchs et al. 10.1073/pnas.1322085111

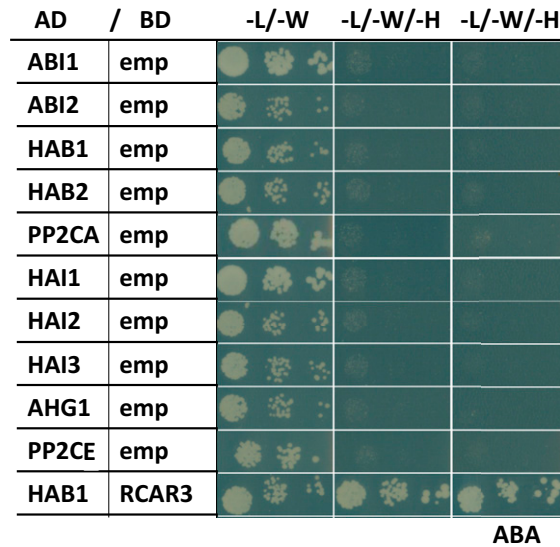


Fig. S1. Regulatory component of abscisic acid (ABA) receptor (RCAR) interaction with protein phosphatases 2C (PP2Cs). Controls of yeast two-hybrid analysis of RCAR7 interaction with all nine clade A PP2Cs. The analysis of histidine-autotrophic growth (-H) is presented for yeasts expressing PP2Cs in the activation domain (AD) and containing the empty DNA-binding cassette (BD, emp) in the absence and presence of 30 μ M ABA. PP2CE-emp and HAB1-RCAR3 served as negative and positive controls, respectively.

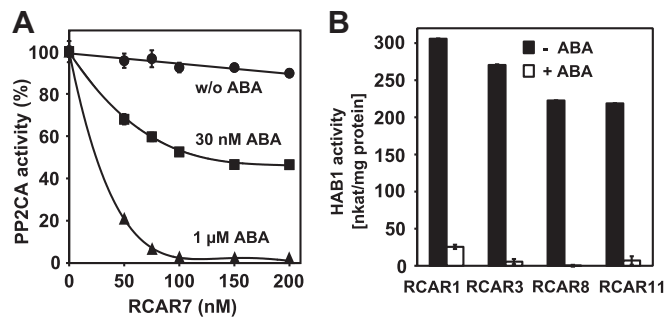


Fig. S2. Regulation of HAB1 phosphatase activity by RCARs. (A) RCAR7-mediated inhibition of PP2CA (50 nM). The activity of PP2CA in the absence of ABA and RCAR7 was set to 100% (0.45 μ kat/mg protein). (B) RCAR1-, RCAR3-, RCAR8-, and RCAR11-mediated inhibition of HAB1 phosphatase activity in the presence and absence of 1 μ M ABA. HAB1 protein (50 nM) was incubated in the presence of a twofold molar excess of RCAR (mean \pm SD).

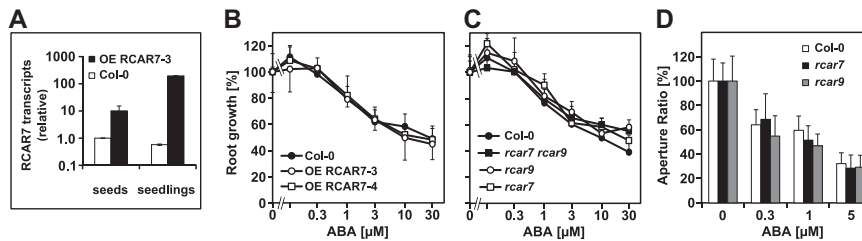


Fig. S3. RCAR7 expression and ABA responses of *Arabidopsis* with altered RCAR7 expression. (A) RT-PCR analysis of RCAR7 transcript levels in seeds, imbibed for 1 d, and 4-d-old seedlings from wild type (Col-0) and an RCAR7-overexpressing (OE) line. RCAR7 transcript levels were normalized to ubiquitin 10 expression, and 0.4% of ubiquitin 10 transcript abundance was reached in wild-type seeds (set to 1). (B) Inhibition of root growth of RCAR7-overexpressing lines in the presence of ABA (3 d; $n > 10$ per data point). In the absence of ABA, root growth equaled 19.2 ± 3.0 mm, 17.2 ± 2.4 mm, and 19.2 ± 0.7 mm for OE RCAR7-3, OE RCAR7-4, and the control line, respectively. (C) Analysis as shown in B for *rcar7*, *rcar9*, and the double mutant *rcar7rcar9* in comparison with Col-0. In the absence of ABA, root growth equaled 14.0 ± 1.9 mm, 16.8 ± 2.2 mm, 14.8 ± 0.5 mm, and 15.3 ± 1.8 mm for *rcar7*, *rcar9*, *rcar7rcar9*, and the control line, respectively (mean \pm SD). (D) Stomatal response of 2-wk-old plants of the knockout lines exposed to ABA ($n > 20$ per data point, two-way ANOVA Tukey test).

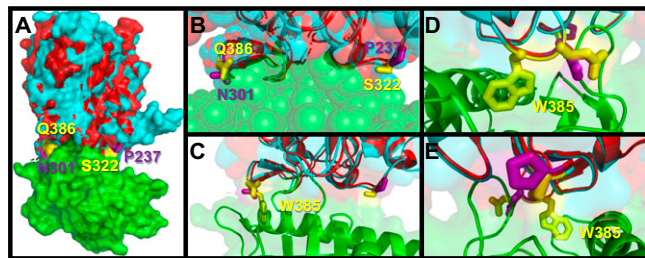


Fig. S4. Structural overlay of HAB1–RCAR11 and ABI1–RCAR12 receptor complexes. (A) HAB1 (cyan) and ABI1 (red) in complex with RCAR11 and RCAR12 (green) based on Protein Data Bank ID codes 3QN1 and 3KDJ, respectively. Two amino acid residues of HAB1 found to be critical for the interaction with RCAR7 are located at the periphery of the interaction surface and are highlighted in yellow (S322, Q386), whereas the corresponding residues in ABI1 (P237, N301) are shown in violet. (B) Close-up of the interaction site. The interaction surface of HAB1 and ABI1 with the ABA receptors is structurally similar, as indicated by the largely overlapping positions of the amino acid residues (cyan and red spheres) and the PP2C protein backbones (cyan and red lines). The side chains of P237, N301 and S322, Q386 are shown. (C) View similar to B highlighting the protein secondary structure (helix, β -sheet) and a critical tryptophan residue of the PP2Cs (W385 in HAB1, shown in yellow), which interlocks with the RCAR and contacts the ABA ligand (not shown for clarity). The functionally important tryptophan is adjacent to the residues Q386 and N301 of HAB1 and ABI1, respectively. (D and E) Close-up and perpendicular view of C showing Q386/N301 (D) and S322/P237 (E) in front and the W385 of HAB1.